ACS OMEGA

Open Access

http://pubs.acs.org/journal/acsodf

Article

Flowable Oxygen-Release Hydrogel Inhibits Bacteria and Treats Periodontitis

Feng Wang, Shengnan Wei, Jingya He, Aili Xing, Yuan Zhang, Zhongrui Li, Xiangxiang Lu, Bin Zhao,* and Bin Sun*

Cite This: *ACS Omega* 2024, 9, 47585−47596

Read Online

ACCESS | Metrics & More | Article Recommendations

ABSTRACT: Periodontitis, the chronic inflammation of the periodontal tissues caused by bacteria in plaque, is the leading cause of tooth loss in adults in the world. Currently, periodontitis is effectively treated with mechanical cleaning and the use of antibiotics. However, these treatments only temporarily remove plaque, which can rapidly proliferate and multiply in periodontal pockets over time. Although antibiotics have positive antimicrobial effects, their long-term use increases the risk of the emergence of drug-resistant strains. The emergence of resistant strains reduces the effectiveness of periodontitis treatment and makes the disease more difficult to control. Herein, this paper reports the development of an injectable self-oxygenating composite hydrogel for periodontal therapy, which was produced by loading CaO_2 nanoparticles and ascorbic acid into an injectable alginate hydrogel. CaO_2 can improve the periodontal pocket microenvironment by reacting with water to generate oxygen, calcium ions can be used as a bone regeneration material, and ascorbic acid protects cells. The authors further showed that the composite hydrogel inhibited growth and colonization of anaerobic bacteria, reduced the degree of inflammation, and promoted alveolar bone regeneration. In conclusion, these findings suggest that the composite hydrogel can be used as a biocompatible, convenient, and effective method for periodontitis treatment.

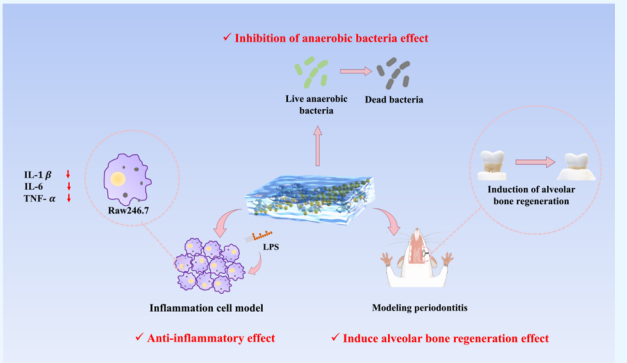

INTRODUCTION

Periodontitis is the chronic inflammation of periodontal tissue caused by bacteria in subgingival plaque and is a common disease of the oral cavity.[1] A total of 538 million people worldwide suffer from severe periodontal disease, and 276 million have lost their teeth as a result. These numbers will continue to increase as the population grows and ages.[2] The early manifestations of periodontitis are redness and swelling of the gums and infiltration of periodontal tissue by neutrophils followed by destruction of periodontal connective tissue, formation of periodontal pockets, and resorption of alveolar bone, leading to the loosening and loss of teeth. The pathogenesis of periodontitis depends critically on the attack of pathogenic bacteria on the body and the consequent autoimmune response of the body.[3,4] Periodontitis is currently the leading cause of tooth loss in adults worldwide and seriously affects the physical and mental health of patients.

The current treatment of periodontitis is mainly to remove plaque and tartar from periodontal pockets by mechanical methods such as supragingival scraping and subgingival scraping supplemented by antibiotic treatment. The broad use of antibiotics can lead to bacterial resistance, which reduces the efficacy of antibiotics and ultimately affects the treatment outcome.[5] Therefore, the development of a new nonantibiotic antiplaque drug is essential. The plaque in periodontal pockets is mainly Gram-negative anaerobic bacteria, such as *Porphyromonas gingivalis* (*P. gingivalis*) and *Fusobacterium nucleatum* (*F. nucleatum*).[6] Anaerobic bacteria are sensitive to oxygen content, and increasing the oxygen content can significantly inhibit the growth of anaerobic bacteria,[7] Therefore, an oxygen-producing drug could be developed to inhibit and kill anaerobic bacteria in subgingival plaque. In addition, increasing the oxygen content can also promote the regeneration of bone tissue[8] and facilitate the regeneration of periodontal tissue. In summary, strategies that can be used to increase the oxygen content of periodontal pockets with oxygen-producing drugs may be effective in the treatment of periodontitis.

An ideal oxygen-releasing material should have sustainable oxygen release properties, low toxicity, and high biocompat-

Received: July 18, 2024
Revised: October 1, 2024
Accepted: October 4, 2024
Published: November 20, 2024

https://doi.org/10.1021/acsomega.4c06642
ACS Omega 2024, 9, 47585−47596

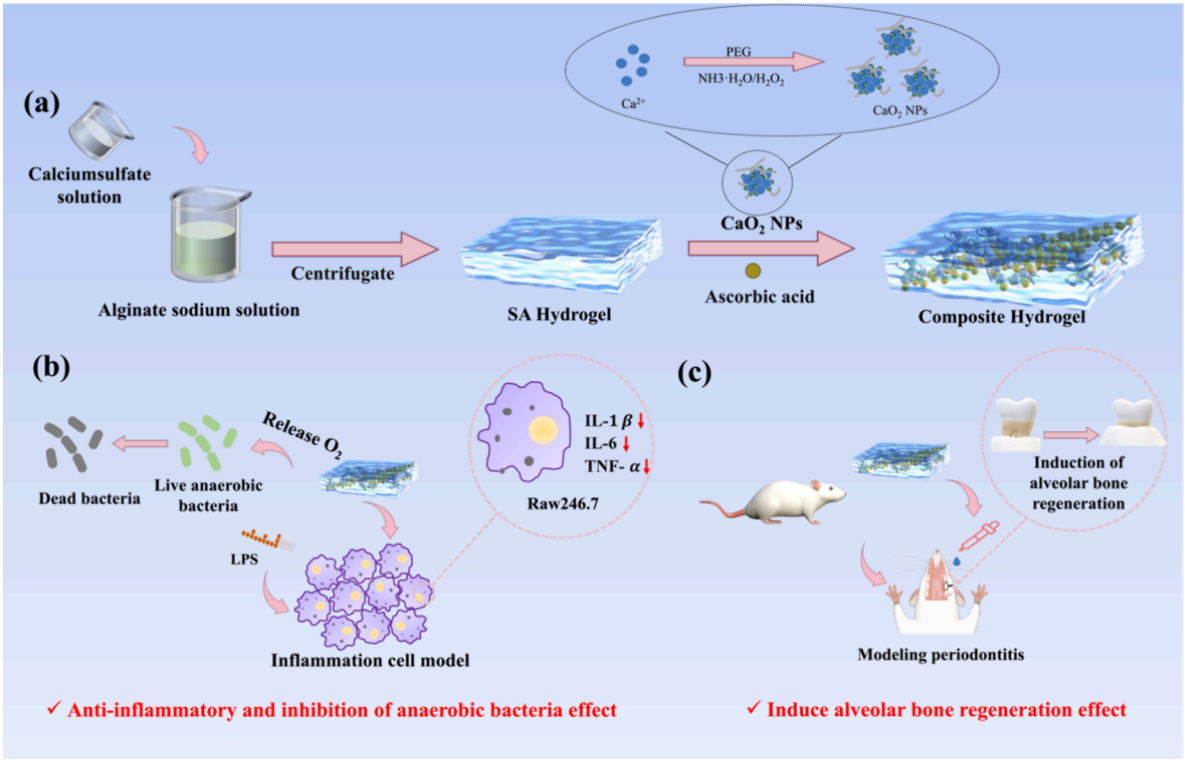

Figure 1. Preparation process of the composite hydrogel and schematic illustration of the antimicrobial and anti-inflammatory effects *in vitro* and the promotion of alveolar bone regeneration *in vivo*. (a) Process for making the injectable composite hydrogel. (b) Schematic diagram of the composite hydrogel for anaerobic bacteria inhibition and anti-inflammation. (c) The composite hydrogel promotes alveolar bone regeneration effect.

ibility. Oxygen-releasing materials can be divided into two types: The first is oxygen-producing materials, which produce oxygen through chemical reactions; the most common oxygen-producing materials are peroxides, such as calcium peroxide (CaO_2), magnesium peroxide (MgO_2), and sodium percarbonate (SPO). The second is oxygen-carrying materials, which do not produce oxygen,[9] such as perfluorinated carbons (PFC) emulsions,[10,11] PFC-cyclodextrin complexes,[12] hemoglobin particles,[13] fluorinated zeolite particles,[14] and polymers encapsulating PFC.[15,16] As a commonly used solid oxygen-producing material, CaO_2 has been studied more frequently in oxygen-releasing systems of peroxides. CaO_2 has a long oxygen release time and dissolution rate between SPO and MgO_2,[17] and calcium ions can be used as a raw material for bone regeneration. Therefore, CaO_2 was chosen as the drug to provide oxygen in the periodontal pocket.

When CaO_2 meets water, it condenses into clumps, which affects the rate of oxygen release. In 2017, Liu et al. utilized the hydrophobic cavity and hydrophobic layer of liposomes loaded with methylene blue and CaO_2 nanoparticles (NPs) to construct a self-oxidizing LipoMB/CaO_2.[18] In 2019, Zhang et al. synthesized PCL/CaO_2 composite microspheres using polycaprolactone (PCL) as a CaO_2-containing matrix, which ensured the CaO_2 steady state without affecting the oxygen release function.[19] Therefore, limiting the contact of CaO_2 with water is an effective solution. Based on the above ideas, this study uses biodegradable materials as the matrix and wraps CaO_2 as the oxygen source, which avoids the agglomeration problem of CaO_2 without affecting the oxygen production efficiency. Consequently, we synthesized the sodium alginate (SA) hydrogel,[20] endowed it with mobility to injection into periodontal pockets, and successfully loaded CaO_2 NPs into the SA hydrogel. Encapsulation of CaO_2 NPs in a hydrogel limits its exposure to water, thereby controlling the rate of oxygen release.

Hydrogels are three-dimensional networks characterized by high water content and absorption properties; they are composed of large molecular polymers, which exhibit excellent biocompatibility. These materials can be classified into two main categories: natural hydrogel polymers and synthetic hydrogel polymers.[21,22] Although natural hydrogels demonstrate favorable biocompatibility, safety, and nontoxicity, they also present limitations such as poor solubility in water, inadequate mechanical strength, and insufficient stability—factors that constrain their application in the biomedical field to some extent. In recent years, significant advancements have been made in the development of synthetic hydrogels; these artificially synthesized materials not only retain the inherent advantages of natural hydrogels but also mitigate their shortcomings, thereby enhancing the overall applicability of hydrogels.[23−26] Nanoparticles, owing to their diminutive size, enhance penetration and biointeraction at the wound site. Their high specific surface area facilitates cell adhesion, thereby expediting the healing process of various wounds or ulcers. Hydrogel serves as a porous scaffold capable of encapsulating drugs or biomolecules. By integrating these two materials to create a composite platform known as a nanocomposite hydrogel, researchers have employed diverse nanomaterials to develop multifunctional hydrogels exhibiting pronounced antibacterial, anti-inflammatory, and antioxidant properties.[27−29]

https://doi.org/10.1021/acsomega.4c06642
ACS Omega 2024, 9, 47585−47596

Considering that CaO_2 reacts with water to form calcium hydroxide, which is an alkaline product, we added ascorbic acid to the hydrogels. Ascorbic acid is an acidic antioxidant; on the one hand, it can inhibit the excess hydrogen peroxide, reduce the production of reactive oxygen species, and avoid the damage of cellular DNA and proteins; on the other hand, it can regulate the acid−base imbalance induced by calcium hydroxide and avoid the cell death caused by calcium overload. In addition, ascorbic acid can reduce the toxicity of the hydrogel and promote the survival of cells encapsulated in hydrogels.[30−32]

Here, based on the oxygen-producing capacity of CaO_2 NPs and the antioxidant capacity of ascorbic acid, we utilized a highly mobile SA hydrogel as a carrier, thus creating an injectable composite hydrogel (Figure 1a). The hydrogel has good fluidity to be injected into periodontal pockets, and the loaded CaO_2 NPs and ascorbic acid can kill anaerobic bacteria, promote alveolar bone regeneration, and inhibit the development of inflammation (Figure 1b,c), which can be used for the treatment of periodontitis. The SA hydrogel can be degraded slowly, which avoids the problem of CaO_2 NPs clumping while guaranteeing the function of the drug. The favorable *in vitro* cell compatibility and *in vivo* biocompatibility further substantiate the overall biocompatibility of the hydrogel. In conclusion, our research findings indicate that composite hydrogels represent a promising and effective therapeutic approach for periodontitis, attributed to their excellent biocompatibility, user-friendliness, and efficacy.

EXPERIMENTAL SECTION

Materials and Test Instruments. Calcium chloride (99.5%), hydrogen peroxide (35%), polyethylene glycol, ammonia (25%), sodium hydroxide, calcium sulfate, chloroform, and absolute ethanol were purchased from Beijing Chemical Co., Ltd. Ascorbic acid was purchased from Sigma-Aldrich Reagent Co. Sodium alginate was purchased from Aladdin Reagents, Inc. LIVE/DEAD BacLight TM Bacterial Viability Kits were purchased from Introvigen Reagents. The following instruments were used: cold field emission scanning electron microscope (JSM-6700F, JEOL), infrared spectrometer (FTIR, Nicolet AVATAR 360), GC-7920 vacuum closed gas circulation system gas chromatograph (Beijing Zhongjiao Jinyuan Technology Co., Ltd.), Empyrean X-ray diffractometer (PANalytical B.V., The Netherlands), fluorescence microscope (DP2-BSW, Olympus, Japan), and Micro-CT SCANCO Medical AG HR10 rheometer (TA, USA).

Synthesis of CaO_2 NPs. Six grams of calcium chloride was dissolved in 60 mL of deionized water; 30 mL of 1 mol/L ammonia solution and 240 mL of polyethylene glycol were added and stirred well at room temperature; 30 mL of 30% hydrogen peroxide solution was added; and the pH was adjusted to 10 by adding ammonia solution. The precipitate was dried for 2 h in a vacuum oven at 80 °C to obtain CaO_2 NPs.[33,34]

Synthesis of the Injectable SA Hydrogel. The SA hydrogel was obtained by adding 10 mL of saturated sodium sulfate solution to 10 mL of 1 wt % aqueous sodium alginate solution, mixing well, and centrifuging to remove air bubbles.

Synthesis of the Injectable Composite Hydrogel. Ten milliliters of saturated sodium sulfate solution was added to 10 mL of 1% aqueous sodium alginate solution, and 4 mg of CaO_2 NPs and 6 mg of ascorbic acid were added after mixing and centrifuged to remove the air bubbles. The injectable composite hydrogel loaded with CaO_2 NPs and ascorbic acid was obtained.[35,36]

Characterization of Injectable Composite Hydrogels. The hydrogel was lyophilized, and the morphology was observed by scanning electron microscopy. Then the Fourier transform infrared spectra of CaO_2 NPs, ascorbic acid, sodium alginate hydrogels, and sodium alginate hydrogels loaded with calcium peroxide and ascorbic acid were tested separately, and the presence of each component in the composite hydrogel was confirmed by comparing the characteristic peak positions. Finally, the mechanical properties of the hydrogel were tested by using a rheometer.

Oxygen Production Capacity Testing of Injectable Composite Hydrogels. The composite hydrogel was added to 50 mL of water, evacuated to remove the air, and then passed through a gas collection device and connected to a gas chromatograph to measure the amount of oxygen produced once a day. At the same time, the same hydrogel was placed in several times the volume of neutral water to observe the degradation time and to detect the pH value of the degraded liquid.

***In Vitro* Inhibition of Anaerobic Bacteria.** After introducing the composite hydrogels into the culture medium, *P. gingivalis* and *F. nucleatum* were cocultured anaerobically at 37 °C (*P. gingivalis* for 72 h and *F. nucleatum* for 24 h). During the logarithmic phase, the bacterial mixture was spread onto Columbia blood agar plates and incubated in an anaerobic environment at 37 °C. Subsequently, the same procedure was repeated using a pure culture medium and SA hydrogels instead of composite hydrogels.

Staining of Live/Dead Bacteria. The bacterial solution in the logarithmic phase mentioned above was stained with NucGreen and EthD-III. The mixture was observed, and images were captured using a laser confocal microscope utilizing an FITC filter to visualize green fluorescence as indicative of live bacteria while employing a PI filter to detect red fluorescence as an indication of dead bacteria.

Biosafety of the Composite Hydrogel. The L929 cells with good cell morphology were taken as the study object; inoculated in 96-well plates at 10^5 cells/well, 100 mL per well; and incubated in a cell incubator at 37 °C and 5% CO_2. The control group, SA hydrogel group, and composite hydrogel group were established. The cells were incubated in a cell incubator at 37 °C with 5% CO_2 for 24 h. After 24 h, the liquid was aspirated, and the cells were rinsed with PBS three times to ensure the removal of residual water. Ninety milliliters of complete medium and 10 mL of CCK-8 solution were added to each well, and the cytotoxicity of the composite hydrogel was calculated by measuring the absorbance of each well at 450 nm after incubation for 2 h protected from light.

Forty-five 6 week old SD rats were randomly divided into the control group, the SA hydrogel group, and the composite hydrogel group (15 rats/group). Each group was then injected with saline, sodium alginate hydrogels, and self-produced oxygen composite hydrogels into the periodontal pockets of the rats once a week. The rats in each group were killed at 4 and 8 weeks (five rats each time). The hearts, livers, spleens, and lungs were fixed in 4% paraformaldehyde solution for histopathological examination, and venous blood was taken from rats for liver and kidney functions.

Establishment of a Cellular Model of Periodontitis. Raw264.7 cells with good cell morphology were taken as the study object; inoculated in 96-well plates at 10^5 cells/mL, 100

https://doi.org/10.1021/acsomega.4c06642
ACS Omega 2024, 9, 47585−47596

mL per well; and placed in a cell incubator at 37 °C with 5% CO_2 for 24 h. After 24 h, it was changed to an H-DMEM without fetal bovine serum. Control and LPS groups were established, in which 100 mL of the complete medium was added to the blank control group, and the concentration of the LPS group was set to 0.1, 0.5, 1, and 2 μg/mL, respectively; 100 mL of configured LPS solution was added to each well, and four replicate wells were set in each group. After 24 h, the cell supernatant was collected and centrifuged to determine the NO content by a Nitric Oxide Assay Kit, and the cells in 96-well plates were used to determine the cell viability by CCK-8 to screen the appropriate LPS modeling concentration.

Anti-inflammatory Effect of the Composite Hydrogel. *Quantitative Real-Time PCR (qRT-PCR) for the Detection of Inflammatory Factor Gene Expression.* Raw264.7 cells were inoculated in six-well plates at a density of 2×10^5 cells/well and placed in a 37 °C, 5% CO_2 incubator for 24 h. After 24 h, the medium was changed to simple H-DMEM, and the cells were starved overnight. Control, LPS, LPS + SA hydrogel (200 mg/mL), and LPS + composite hydrogel (200 mg/mL) groups were established, and the cells were collected 24 h later for RNA extraction. Samples with OD 260/280 values in the range of 1.8−2.0 were screened for reverse transcription to cDNA. Add 1 μg mRNA to the RNase free centrifuge tube, 3 μL 5 μgDNA Digester Mix, then add RNase free H_2O to 15 μL, centrifuge quickly and briefly, and 42 °C incubation for 2 min. The obtained mRNA was reverse transcribed. The 4× Hifair III SuperMix plus was added directly to the reaction tube in step 1, and after fast and brief centrifugation, the reaction was incubated at 25 °C for 5 min, 55 °C for 15 min, and 85 °C for 5 min for reverse transcription. The primers were designed and synthesized by Shanghai Biotechnology Company, and the primer sequences are shown in Table 1. The qRT-PCR reagent ratios and machine settings are as in Tables 2 and 3.

Table 1. Primer Sequences

gene name	primer sequences
IL-1β	F: TCCAGGATGAGGACATGAGCAC
TNF-α	R: GAACGTCACACACCAGCAGGTTA
IL-6	F: CTCATGCACCACCACCAAGGACTC
	R: AGACAGAGGCAACCCGACCACTC
	F: GAACGTCACACACCAGCAGGTTA
	R: CCAGTTTGGTAGCATCCATCATTTC

Table 2. qRT-PCR System

reagents	20 μL reaction system (μL)	final concentration
Hieff qRT-PCR SYBR Green Master Mix (Low Rox Plus)	10	1×
		0.2 μM
forward primer (10 μM)	0.4	0.2 μM
reverse primer (10 μM)	0.4	
template DNA	0.6	
DEPC water	8.6	

Detection of Secreted Proteins in Cell Supernatants by an Enzyme-Linked Immunosorbent Assay (ELISA). The cells were cultivated as described above, and the cell supernatant was collected. The standard, zero, and experimental group wells were prepared. The reaction wells were sealed with a plate sealing mold and incubated at 37 °C for 2 h. The liquid was discarded, and the supernatant was dried and washed four times by adding washing solution. The detection antibody (100 μL) was added and incubated at 37 °C for 1 h; after washing four times, 100 μL of HRP-labeled streptavidin was added and incubated at 37 °C for 40 min; after washing four times, 100 μL of TMB chromogenic solution was added to each well; 100 μL of TMB color development solution was added to each well and incubated at 37 °C for 15 min away from light; 100 μL of termination solution was added, and the absorbance of each well was measured at 450 nm. The standard curve was calculated and plotted according to the standard curve equation to calculate the concentration value in each experimental group.

Table 3. PCR Conditions

cycle steps	temperature	time	number of cycles
predenaturation	95 °C	5 min	1
denaturation	95 °C	10 s	40
annealing/extension	60 °C	30 s	40
dissolution curve stage	instrument default settings		1

Therapeutic Efficacy of Composite Hydrogels in a Periodontitis Rat Model. Forty-five 6 week old SD rats were randomly divided into a control group, an SA hydrogel group, and a self-produced oxygen composite hydrogel group (15 rats/group). The necks of the left maxillary second molars were ligated and removed after 2 weeks to create a rat model of periodontitis, and then each group was injected with saline, SA hydrogels, and self-produced oxygen composite hydrogels into the periodontal pockets of rats once a week. The rats in each group were executed at 4 and 8 weeks after the operation (five rats each time). The maxillae of rats were taken and fixed in a 4% paraformaldehyde solution for histopathology and micro-CT analysis.

Statistical Analysis. The data of this experiment were analyzed using GraphPad Prism 9 software, and the resultant data were expressed as mean ± SD. The data of each experiment conformed to the normal distribution with chi-square variance. $p < 0.05$ (*), $p < 0.01$ (**), and $p < 0.001$ (***) were used to represent statistical difference. Images and fluorescence intensities were processed or analyzed by the ImageJ software.

RESULT AND DISCUSSION

Synthesis and Characterizations of the Composite Hydrogel. Periodontal pockets in patients with periodontitis are small and differently shaped, making it difficult for drugs to be inserted into them. Hydrogels with a certain fluidity can be injected directly into the periodontal pockets, which are ideal for intrapocket drug delivery. We synthesized a hydrogel with a certain degree of fluidity by modifying the cross-linking state of the SA hydrogels. As shown in Figure 2a, this composite hydrogel is flowable and will flow when the container is tilted or inverted.

The morphology of SA hydrogels[20] and composite hydrogels was analyzed using scanning electron microscopy(SEM) after freeze-drying. The SEM reveals a distinct porous structure in both hydrogels. Further element distribution analysis showed that carbon, oxygen, and sodium were evenly distributed in both types of hydrogels, confirming that SA is the main component of both hydrogels (Figure 2c). The results also confirmed the uniform distribution of sulfur and calcium in the hydrogel skeleton for the other major component, calcium

https://doi.org/10.1021/acsomega.4c06642
ACS Omega 2024, 9, 47585−47596

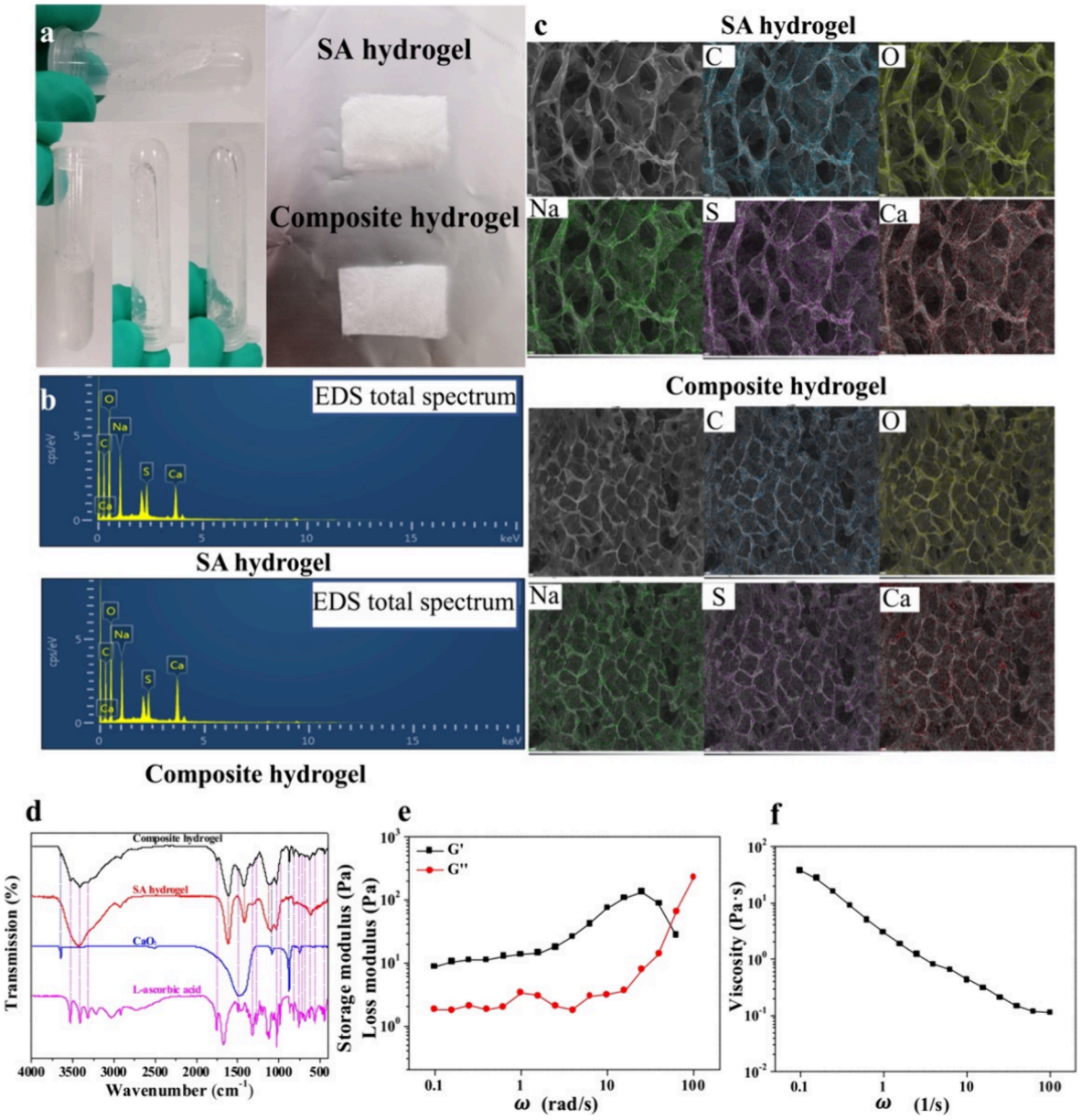

Figure 2. (a) Hydrogel exists as a fluid at ambient temperature and transitions to a solid state following freeze-drying. (b) EDS total spectrum of the SA hydrogel and composite hydrogel. (c) SEM images of the SA hydrogel and composite hydrogel. The scale bar is 100 μm. (d) FITR spectra of L-ascorbic acid, CaO_2, SA hydrogel, and composite hydrogel. (e) Rheological analysis of the composite hydrogel. (f) Viscosity test of the composite hydrogel.

sulfate. The elemental composition analysis of the hydrogel based on the characteristic energy of X-ray photons confirmed the presence of carbon, oxygen, sodium, sulfur, and calcium (Figure 2b). We further compared the overall elemental mass fraction of the two hydrogels. The change in elemental mass fraction in the composite hydrogels, as compared to that of the SA hydrogels, indicates the successful loading of CaO_2 NPs and ascorbic acid, particularly evidenced by an increase in calcium content from 3.64 to 5.46% (Table 4).

The composite hydrogel was supplemented with ascorbic acid to provide cellular protection. The Fourier transform infrared (FTIR) spectra presented in Figure 2d reveal characteristic peaks associated with sodium alginate hydrogels, calcium peroxide, and ascorbic acid, thereby confirming the successful integration of these three components into the composite hydrogels. The mechanical properties of the

Table 4. Elemental Mass Fraction

chemical elements	SA hydrogel	composite hydrogel
C	22.61%	21.93%
O	66.56%	65.39%
Na	5.13%	5.23%
S	2.07%	1.99%
Ca	3.64%	5.46%

hydrogel were assessed by using a rheometer, as depicted in Figure 2e. The storage modulus of the sample exceeds that of the loss modulus, thereby confirming the successful synthesis of the hydrogel. Nevertheless, the comparatively lower storage modulus suggests that the hydrogel exists in a weak gel state. At sufficiently high shear frequencies, an intersection between the storage and loss moduli was observed, indicating a

https://doi.org/10.1021/acsomega.4c06642
ACS Omega 2024, 9, 47585−47596

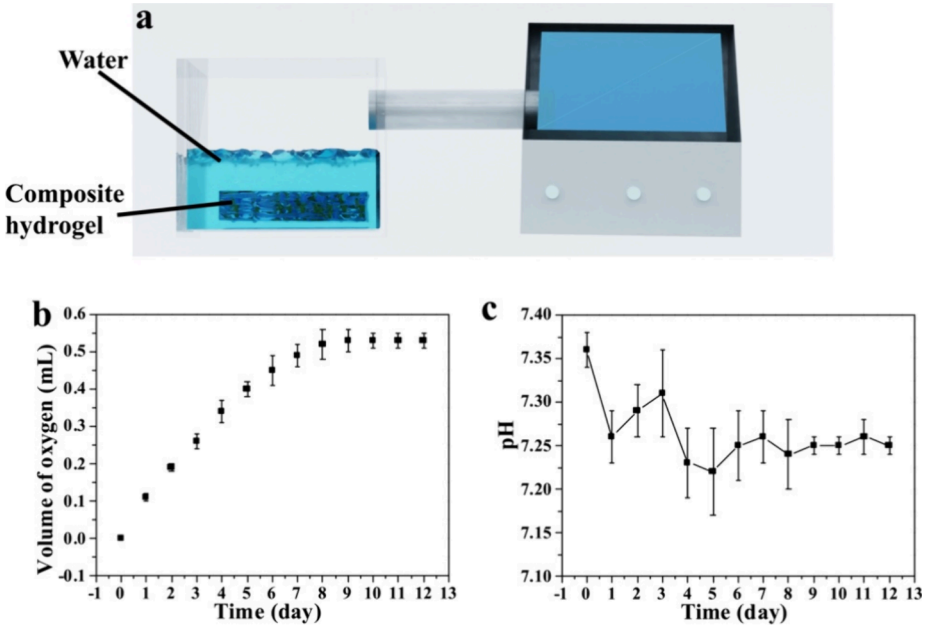

Figure 3. (a) A schematic diagram is presented for the assessment of oxygen generation and degradation performance in the composite hydrogel. (b) The oxygen content has exhibited a gradual upward trend over the past 8 days; however, no significant fluctuations were observed during the subsequent 8 day period. (c) The pH value of degradation products remained neutral, closely resembling the physiological pH of body fluids.

transition from gel to solution phase. At this critical point, structural integrity is compromised, exhibiting characteristics typical of a solution. The viscosity of the composite hydrogel was further investigated. As illustrated in Figure 2f, an increase in cutting frequency leads to a progressive reduction in viscosity, thereby exemplifying the phenomenon of shear thinning.

The storage modulus of the sample exceeds that of the loss modulus, thereby confirming the successful synthesis of the hydrogel. Nevertheless, the comparatively lower storage modulus suggests that the hydrogel exists in a weak gel state. At sufficiently high shear frequencies, an intersection between the storage and loss moduli was observed, indicating a transition from gel to solution phase. At this critical point, structural integrity is compromised, exhibiting characteristics typical of a solution.

Revising the Assessment of Oxygen Generation Capability. In patients with periodontal disease, the presence of reduced oxygen levels within the periodontal pockets facilitates the proliferation of anaerobic bacteria. The composite hydrogel exhibits the ability to generate oxygen and effectively inhibit the growth of anaerobic pathogenic bacteria. To evaluate its efficacy in oxygen generation, gas chromatography was employed (Figure 3a). The findings (Figure 3b) demonstrate that the composite hydrogel consistently generates oxygen over a period of 8 days. The production of oxygen exhibited a noticeable decline after a span of 8 days. Similarly, the composite hydrogel should exhibit excellent biodegradability, thereby enabling precise control over the rate of oxygen release. The hydrogel was observed to undergo continuous degradation with complete degradation achievable within a span of 8−10 days (Figure 3c). Analysis of the pH level in the solution containing the degradation products revealed that it maintained a pH range of 7.2 to 7.4, closely resembling the physiological pH of the human body.

Inhibition of Anaerobic Bacteria *In Vitro*. Gram-negative pathogenic bacteria in subgingival plaque in periodontal pockets are important in the development of periodontitis, and their causative organisms include *P. gingivalis*, *F. nucleatum*, etc.[37,38] The oxygen partial pressure in the gingival sulcus fluid and periodontal pockets of patients with periodontitis is low, which favors the colonization of specific microbial flora such as anaerobic bacteria, which may lead to an imbalance in the host's internal homeostasis, inducing a destructive inflammatory process and affecting the host's immune system.[39] The antibacterial effects of composite hydrogels were investigated by testing two distinct bacterial strains: *P. gingivalis* and *F. nucleatum*.

After incorporating two hydrogels into the *P. gingivalis* medium and incubating for 72 h, the impact of SA hydrogels on the quantity of colony forming units (CFU) can be disregarded, whereas there were almost no surviving bacteria in the composite hydrogel group (Figure 4a). This phenomenon may be attributed to oxygen generation by the composite hydrogels upon reaction with water, thereby impeding *P. gingivalis* growth. To further verify the antibacterial performance of the system against other anaerobic bacterium in the oral cavity, we selected *F. nucleatum* as representatives. The composite hydrogel significantly reduced the number of *F. nucleatum* after 24 h of treatment (Figure 4b). These findings highlight the broad-spectrum antibacterial activity of the composite hydrogel against anaerobic bacteria.

To further investigate the inhibitory effect of the composite hydrogel on anaerobic bacteria, we performed live/dead staining assays and observed the samples using a laser scanning confocal microscope. As depicted in Figure 4c, the SA hydrogel group exhibited a substantial presence of viable *P. gingivalis*, while the composite hydrogel group displayed a significant proportion of nonviable bacteria with minimal live bacterial count. Similar results were observed for *F. nucleatum* fluorescence statistics on the percentage of live and dead bacteria (Figure 4d). After conducting statistical analysis, it was

https://doi.org/10.1021/acsomega.4c06642
ACS Omega 2024, 9, 47585−47596

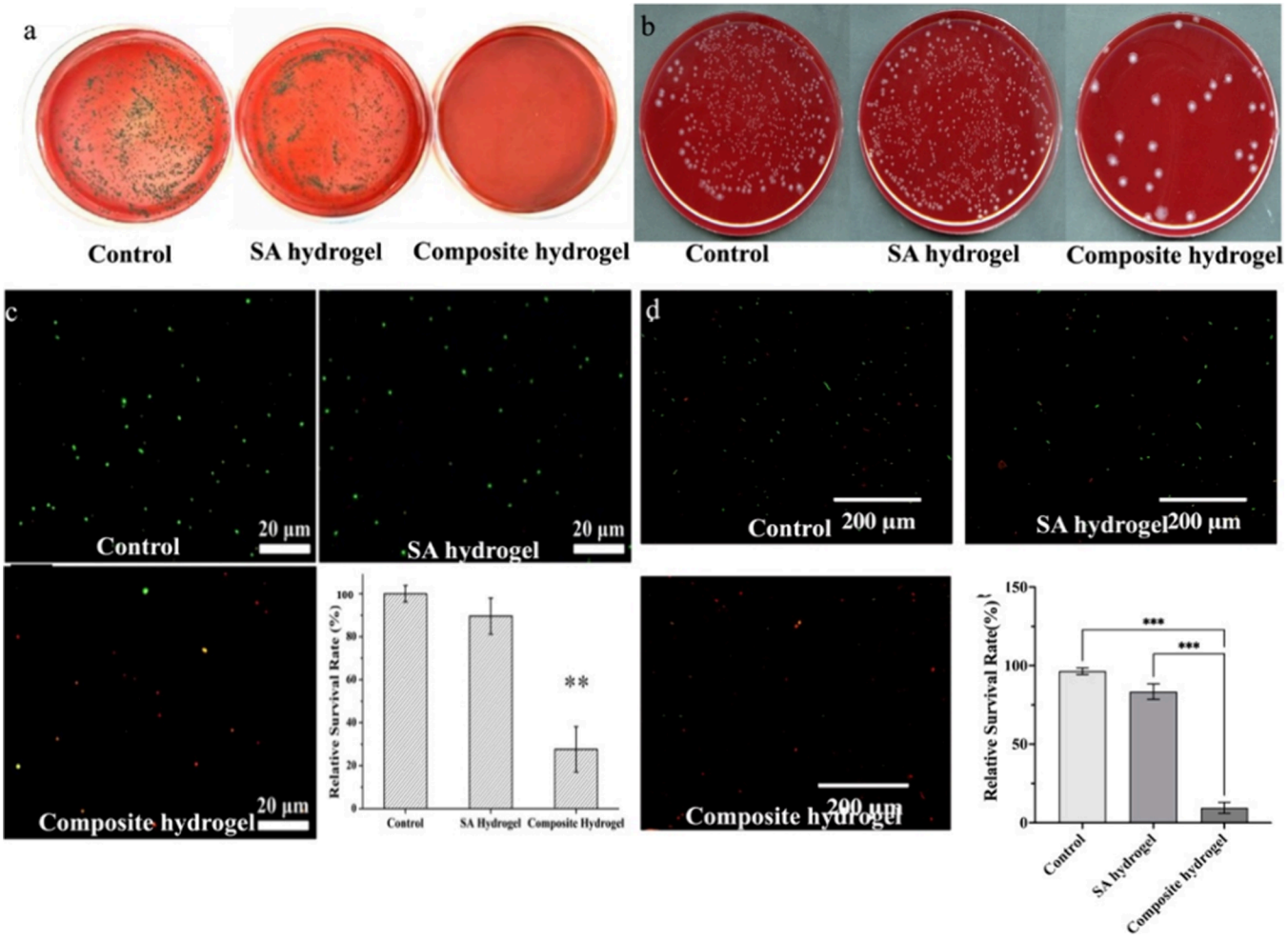

Figure 4. (a, b) The inhibitory effects of the composite hydrogel on *P. gingivalis* and *F. nucleatum* were observed by quantifying CFU. (a) *P. gingivalis*, (b) *F. nucleatum*. (c, d) Bacteriostatic action of the SA hydrogel and composite hydrogel. Green fluorescence represents living bacteria, red fluorescence represents dead bacteria, and three groups of green fluorescent areas were used to quantitatively compare the bacteria survival rate. (c) *P. gingivalis*. (d) *F. nucleatum*. $^{**}P < 0.01$.

determined that the composite hydrogel group exhibited approximately 24.5% viability of *P. gingivalis* (Figure 4c), whereas the composite hydrogel group demonstrated around 9.5% viability of *F. nucleatum* (Figure 4d). These findings suggest that the composite hydrogel possesses potent antimicrobial properties against anaerobic bacteria.

Biosafety of the Composite Hydrogel. The biocompatibility of biomaterials plays a pivotal role in their application. Histopathological examination of the major organs in rats was conducted to assess the potential toxicity of this hydrogel. The picture in Figure 5a shows the effects of the control group and SA hydrogel group as well as the composite hydrogel group on different organs. The SA hydrogel group and composite hydrogel group exhibited no significant histopathological abnormalities in the major organs (heart, liver, spleen, lungs, and kidneys) as observed in the H&E-stained tissue sections when compared to the control group. The blood samples of rats were collected to assess liver and kidney function. As depicted in Figure 5c–f, no significant differences were observed in the key functional parameters of the liver and kidney between the control group, the SA hydrogel group, and the composite hydrogel group, including bilirubin, uric acid, creatinine, albumin, serum globulin, total protein, transferase enzymes, alkaline phosphatase levels, serum electrolytes (phosphorus, magnesium, calcium), and bicarbonate concentrations. To further evaluate the cytocompatibility of these hydrogels, a direct contact test between the L929 cells and hydrogels was carried out. The results demonstrated that neither the SA hydrogel nor the composite hydrogel at various concentrations (100–500 mg/mL) exhibited any discernible impact on the viability of L929 cells (Figure 5b).

Anti-inflammatory Effect of the Composite Hydrogel. In the progression of periodontitis, inflammatory factors, such as interleukin-6 (IL-6), IL-1β, and tumor necrosis factor-alpha (TNF-α), play a pivotal role in the degradation of periodontal tissues.[40] Several scholars have observed a significant elevation in the level of IL-6 within the gingival crevicular fluid of patients diagnosed with chronic periodontitis.[41,42] Accumulating evidence suggests that IL-6 plays a crucial role in the initiation of the early inflammatory response in periodontitis by promoting osteoclast genesis and subsequent bone resorption.[43,44] Likewise, there have been investigations demonstrating a correlation between levels of IL-1β and the severity of periodontitis.[45,46] TNF-α can be detected in both the gingival crevicular fluid and serum of patients suffering from chronic periodontitis.[47,48] Previous studies have demonstrated that TNF induces apoptosis in gingival epithelial cells and fibroblasts while also inhibiting extracellular matrix

https://doi.org/10.1021/acsomega.4c06642
ACS Omega 2024, 9, 47585−47596

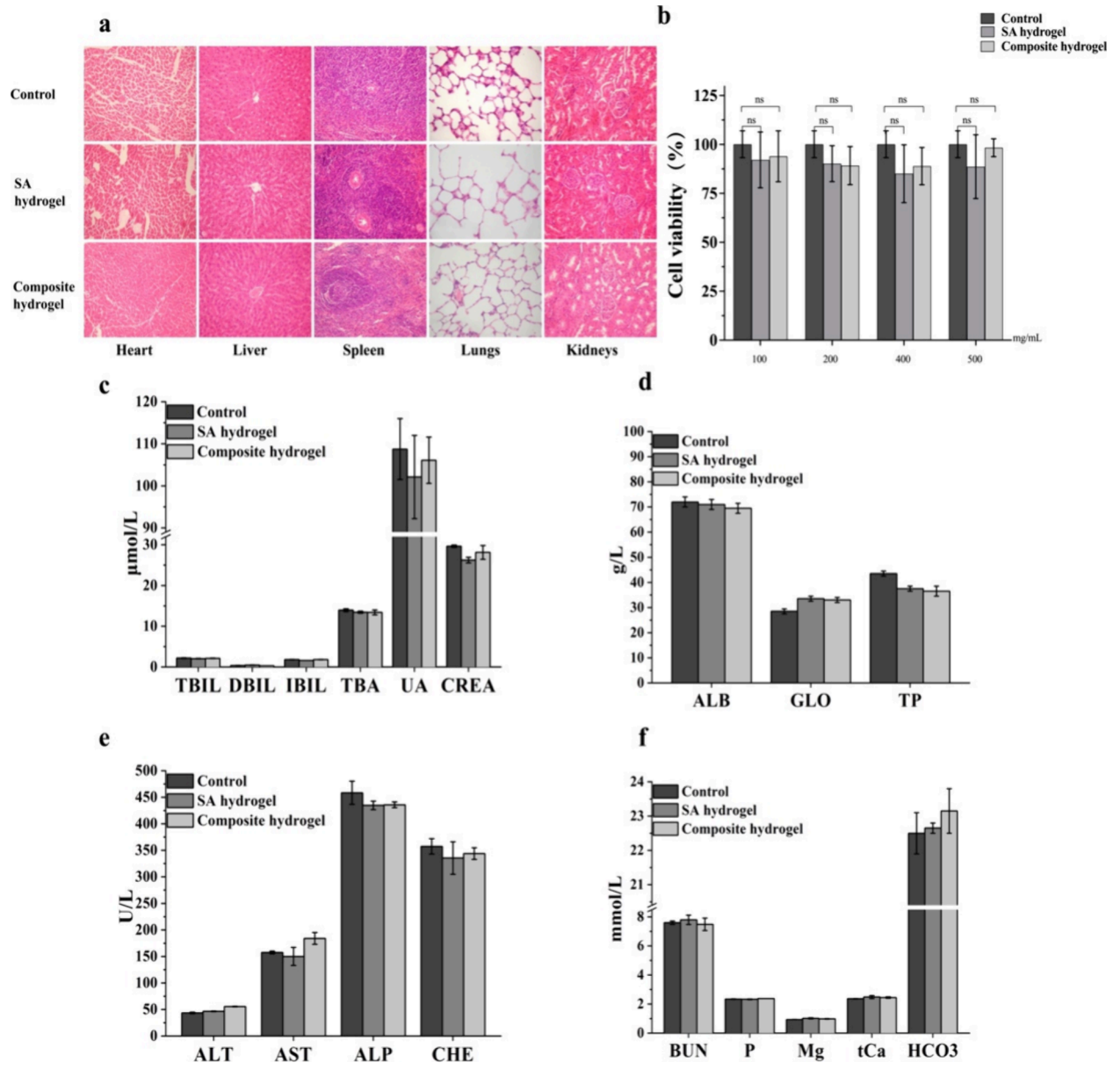

Figure 5. (a) Histopathological examination of the heart, liver, spleen, lung, and kidney was conducted in each experimental group. (b) Effect of the SA hydrogel and composite hydrogel on L929 cell viability. (c–f) Functional evaluations of the liver and kidney in every group. ns: not statistically significant.

production by periodontal fibroblasts,[49,50] thus suggesting its involvement in oral mucosal damage and initiation of periodontitis. Therefore, reducing the secretion of inflammatory factors by cells in an inflammatory state has significant implications for the treatment of inflammation. Investigating the protective effect of composite hydrogels on mouse macrophages (Rwa264.7) under lipopolysaccharide (LPS)-induced inflammatory conditions and exploring their potential for medical applications in inflammatory diseases. Upon direct contact of LPS with Rwa264.7 cells, we observed no significant difference in the amount of nitric oxide (NO) production induced by LPS at various concentrations. The cell viability of Rwa264.7 cells remained unaffected by LPS concentrations ranging from 0 to 1 μg/mL. However, a concentration of 2 μg/mL significantly inhibited cell growth. Consequently, we selected a concentration of 1 μg/mL for inducing an inflammation model in Rwa264.7 cells (Figure 6a).

By detecting the mRNA levels of inflammatory factors, one can deduce the corresponding gene expression. The mRNA expression of *IL-1β*, IL-6, and *TNF-α* in Raw264.7 cells was assessed using real-time quantitative PCR (qRT-PCR) in this experiment. The composite hydrogel group exhibited significantly reduced expression of *IL-1β*, *IL-6*, and *TNF-α* mRNA compared to both the SA hydrogel group and positive control group, with no significant difference observed in the negative control group (Figure 6b). To further investigate the secretion of inflammatory factors, the enzyme-linked immunosorbent assay (ELISA) was employed. The concentrations of IL-1β, IL-6, and TNF-α proteins in the composite hydrogel exhibited a significant reduction compared to those observed in the positive control group; however, no statistically significant difference was observed when compared to that of the negative control group (Figure 6c). It has been demonstrated that the aggregation of inflammatory cells in the alveolar bone can be

https://doi.org/10.1021/acsomega.4c06642
ACS Omega 2024, 9, 47585−47596

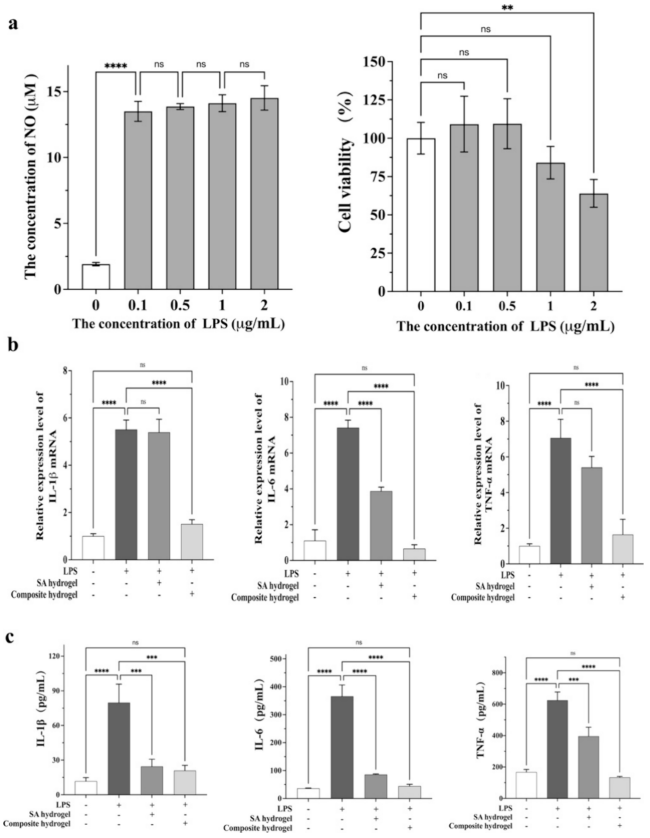

Figure 6. (a) The impact of LPS on NO production and cellular viability in Raw264.7 cells. (b) Effects of the SA hydrogel and composite hydrogel on LPS-stimulated Raw264.7 inflammatory factor mRNA expression. (c) Effect of the SA hydrogel and composite hydrogel on inflammatory factor content in the supernatant of LPS-stimulated Raw264.7 cells. ns: not statistically significant. ***p < 0.001 and ****p < 0.0001.

effectively reduced by local injection of IL-1β, IL-6, and TNF-α receptor blockers in an experimental periodontitis model, which reduced bone resorption by about 60%.[51] The composite hydrogel downregulates the mRNA expression of *IL-1β*, *IL-6*, and *TNF-α* in Raw264.7 cells under an inflammatory state while decreasing *IL-1β*, *IL-6*, and *TNF-α* production. Therefore, the composite hydrogel presented herein demonstrates the capability to mitigate inflammatory responses by effectively reducing the production and secretion of inflammatory cytokines.

Therapeutic Efficacy of Composite Hydrogels in a Periodontitis Rat Model. Patients suffering from periodontitis undergo bone resorption, ultimately resulting in tooth loss. Hence, it is of paramount importance to impede bone resorption and promote regeneration for effective periodontitis treatment. The rat periodontitis model was established through ligature-induced inflammation, and local drug delivery was employed to investigate the therapeutic efficacy of the composite hydrogel in treating periodontitis (Figure 7a). As depicted in Figure 7b, at the 4 week mark, both the control group and SA hydrogel group exhibited evident resorption of the alveolar ridge and reduction in the height of the alveolar crest, resulting in exposure of root bifurcation and intercommunication between sides. However, in the composite hydrogel group, minimal resorption of alveolar bone was observed with only minor exposure to root bifurcation. At 8

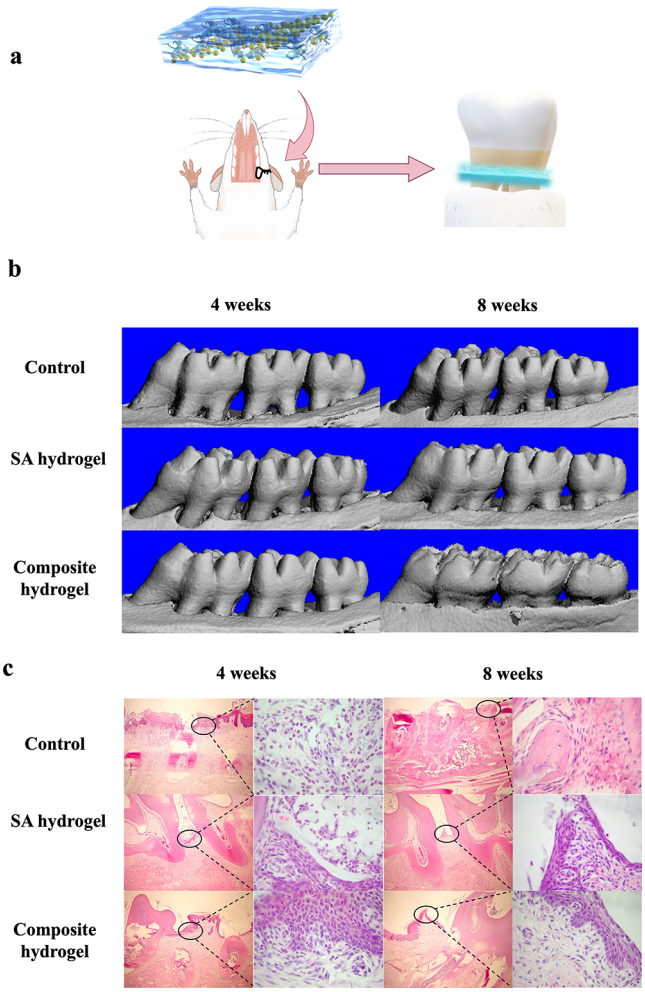

Figure 7. (a) This diagram illustrates the method of applying hydrogels in the periodontal disease model. (b) Micro-CT images of the rat mandible 4 and 8 weeks after the surgery. (c) H&E-stained images of the rat gingiva 4 and 8 weeks after the surgery. All the images were magnified at 40 or 400×.

weeks, both the control group and the SA hydrogel group exhibited a slight improvement in alveolar bone resorption accompanied by gradual elevation of the crest of the alveolar ridge and partial exposure of root bifurcations. In contrast, rats treated with composite hydrogels showed a significant increase in the alveolar bone height, resulting in the complete coverage of root bifurcations by newly formed bone tissue.

Early manifestations of periodontitis are redness and swelling of the gums, vasodilatation, and infiltration of periodontal tissues by neutrophils followed by destruction of periodontal tissues, resorption of alveolar bone, formation of periodontal pockets, and tooth movement. We further examined the gingival tissues of rats by HE staining for inflammation and tissue healing. As depicted in Figure 7c, the control group exhibited disrupted gingival epithelium with a significant infiltration of inflammatory cells at week 4; by week 8, no epithelial repair was observed, and blood vessels remained dilated and infiltrated with inflammatory cells. In the SA hydrogel group, a small amount of epithelial formation and exudation of inflammatory cells were observed at the fourth week; by the eighth week, thinner epithelium without peg formation was evident along with continued inflammatory cell infiltration. Conversely, the composite hydrogel group

https://doi.org/10.1021/acsomega.4c06642
ACS Omega 2024, 9, 47585−47596

displayed thicker epithelial formation with some areas exhibiting epithelial pinnacles and reduced inflammatory cell infiltration at the fourth week; by the eighth week, normal-like epithelial formation with visible pinnacles and decreased inflammatory cell infiltration was observed. The above findings demonstrate the efficacy of composite hydrogels in mitigating periodontal inflammation and facilitating bone regeneration within periodontal tissue.

CONCLUSIONS

In this study, a successful preparation of a sodium alginate hydrogel containing CaO_2 NPs and ascorbic acid was achieved. The hydrogel not only exhibits excellent physical properties but also possesses a variety of potential biomedical applications. Specifically, the hydrogel has a good porous structure, which enables effective promotion of nutrient and gas exchange, providing the necessary growth environment for cells. Additionally, the stable rheological properties ensure the material's operability in practical applications, ensuring that it will not clog or be unevenly distributed during injection or application. From the perspective of degradation performance, the hydrogel exhibits a gradual biodegradation process within the body, facilitating the sustained release of active ingredients. This mechanism aids in maintaining the stability of the local microenvironment and provides continuous therapeutic effects, thereby alleviating the burden of frequent drug administration for patients. Furthermore, the excellent biocompatibility of this material fosters favorable interactions with human tissues, minimizing any significant adverse reactions. Moreover, the hydrogel demonstrated an optimal oxygen release rate attributed to the incorporation of CaO2 NPs, which facilitate oxygen generation through a chemical reaction, thereby enhancing cellular metabolic activity during tissue repair under hypoxic conditions. Studies have indicated that the hydrogel effectively suppresses the expression of key inflammatory mediators, contributing to a reduction in local inflammation. Notably, in a series of experiments encompassing *in vitro* inflammation models and antibacterial efficacy assessments, the hydrogel exhibited significant reductions in inflammatory responses and inhibited the growth and reproduction of anaerobic pathogenic bacteria (including specific oral anaerobes). These findings establish a foundation for clinical applications and suggest that this material may represent a novel therapeutic strategy.

Finally, an 8 week study utilizing a rat model of periodontitis demonstrated the promising therapeutic efficacy of the multifunctional hydrogel in managing this condition. Through careful observation of oral health status, alterations in gingival tissue, and relevant biochemical markers across the experimental groups, it was evident that rats treated with the multifunctional hydrogel exhibited significant improvements compared to those in the control group. These comprehensive findings underscore that a multifunctional hydrogel characterized by fluidity, oxygen-generating capabilities, anti-inflammatory properties, and the potential for bone regeneration represents a vital candidate material for addressing periodontitis and related disorders, thereby providing both theoretical foundations and practical insights for future clinical applications.

ASSOCIATED CONTENT

Data Availability Statement

All animal procedures were performed in accordance with the Guidelines for Care and Use of Laboratory Animals of Jilin University and approved by the Animal Ethics Committee of Jilin University.

AUTHOR INFORMATION

Corresponding Authors

Bin Zhao − *Jilin Provincial Key Laboratory of Tooth Development and Bone Remodeling and Department of Periodontology, Hospital of Stomatology, Jilin University, Changchun 130041, China*; Email: zhaobin2017@jlu.edu.cn

Bin Sun − *Department of Oral and Maxillofacial Surgery, School and Hospital of Stomatology, Jilin University, Changchun 130041, China*; orcid.org/0000-0002-7492-1473; Email: sunbin06@sohu.com

Authors

Feng Wang − *Department of Oral and Maxillofacial Surgery, School and Hospital of Stomatology, Jilin University, Changchun 130041, China; Jilin Provincial Key Laboratory of Tooth Development and Bone Remodeling, Jilin University, Changchun 130041, China*

Shengnan Wei − *Department of Nuclear Medicine, China-Japan Union Hospital, Jilin University, Changchun 130033, China*

Jingya He − *Department of Oral and Maxillofacial Surgery, School and Hospital of Stomatology, Jilin University, Changchun 130041, China; Jilin Provincial Key Laboratory of Tooth Development and Bone Remodeling, Jilin University, Changchun 130041, China*

Aili Xing − *Department of Oral and Maxillofacial Surgery, School and Hospital of Stomatology, Jilin University, Changchun 130041, China; Jilin Provincial Key Laboratory of Tooth Development and Bone Remodeling, Jilin University, Changchun 130041, China*

Yuan Zhang − *Department of Oral and Maxillofacial Surgery, School and Hospital of Stomatology, Jilin University, Changchun 130041, China*

Zhongrui Li − *Department of Oral and Maxillofacial Surgery, School and Hospital of Stomatology, Jilin University, Changchun 130041, China*

Xiangxiang Lu − *Department of Oral and Maxillofacial Surgery, School and Hospital of Stomatology, Jilin University, Changchun 130041, China*

Complete contact information is available at: https://pubs.acs.org/10.1021/acsomega.4c06642

Author Contributions

F.W. executed the experiment and wrote the manuscript. B.S. and B.Z. designed the experiment. All authors edited the manuscript. All authors contributed to the design and implementation of the research and the analysis of results. All authors have seen and approved the final manuscript.

Notes

The authors declare no competing financial interest.

ACKNOWLEDGMENTS

This work was supported by the Jilin Provincial Scientific and Technological Development Program (20210203090SF) and

https://doi.org/10.1021/acsomega.4c06642
ACS Omega 2024, 9, 47585−47596

the National Natural Science Foundation of China (82404401)

REFERENCES

(1) Tonetti, M. S.; Jepsen, S.; Jin, L.; Otomo-Corgel, J. Impact of the global burden of periodontal diseases on health, nutrition and wellbeing of mankind: A call for global action. *J. Clin Periodontol* **2017**, *44* (5), 456−462.
(2) Kassebaum, N. J.; Smith, A. G. C.; Bernabé, E.; Fleming, T. D.; Reynolds, A. E.; Vos, T.; Murray, C. J. L.; Marcenes, W.; GBD 2015 Oral Health Collaborators. Global, Regional, and National Prevalence, Incidence, and Disability-Adjusted Life Years for Oral Conditions for 195 Countries, 1990−2015: A Systematic Analysis for the Global Burden of Diseases, Injuries, and Risk Factors. *J. Dent. Res.* **2017**, *96* (4), 380−387.
(3) Hajishengallis, G. Immunomicrobial pathogenesis of periodontitis: keystones, pathobionts, and host response. *Trends Immunol* **2014**, *35* (1), 3−11.
(4) Hajishengallis, G.; Kajikawa, T.; Hajishengallis, E.; Maekawa, T.; Reis, E. S.; Mastellos, D. C.; Yancopoulou, D.; Hasturk, H.; Lambris, J. D. Complement-Dependent Mechanisms and Interventions in Periodontal Disease. *Front. Immunol.* **2019**, *10*, 406.
(5) Fischer, R. G.; Lira Junior, R.; Retamal-Valdes, B.; Figueiredo, L. C. D.; Malheiros, Z.; Stewart, B.; Feres, M. Periodontal disease and its impact on general health in Latin America. Section V: Treatment of periodontitis. *Braz. Oral Res.* **2020**, *34* (supp1 1), No. e026.
(6) Sharma, A. Persistence of Tannerella forsythia and Fusobacterium nucleatum in dental plaque: a strategic alliance. *Curr. Oral Health Rep* **2020**, *7* (1), 22−28.
(7) Loesche, W. J. Oxygen sensitivity of various anaerobic bacteria. *Appl. Microbiol.* **1969**, *18* (5), 723−7.
(8) Harrison, B. S.; Eberli, D.; Lee, S. J.; Atala, A.; Yoo, J. J. Oxygen producing biomaterials for tissue regeneration. *Biomaterials* **2007**, *28* (31), 4628−34.
(9) Agarwal, T.; Kazemi, S.; Costantini, M.; Perfeito, F.; Correia, C. R.; Gaspar, V.; Montazeri, L.; De Maria, C.; Mano, J. F.; Vosough, M.; Makvandi, P.; Maiti, T. K. Oxygen releasing materials: Towards addressing the hypoxia-related issues in tissue engineering. *Mater. Sci. Eng. C Mater. Biol. Appl.* **2021**, *122*, No. 111896.
(10) Radisic, M.; Park, H.; Chen, F.; Salazar-Lazzaro, J. E.; Wang, Y.; Dennis, R.; Langer, R.; Freed, L. E.; Vunjak-Novakovic, G. Biomimetic approach to cardiac tissue engineering: oxygen carriers and channeled scaffolds. *Tissue Eng.* **2006**, *12* (8), 2077−91.
(11) White, J. C.; Stoppel, W. L.; Roberts, S. C.; Bhatia, S. R. Addition of perfluorocarbons to alginate hydrogels significantly impacts molecular transport and fracture stress. *J. Biomed. Mater. Res., Part A* **2013**, *101* (2), 438−446.
(12) Deluzio, T. G. B.; Penev, K. I.; Mequanint, K. Cyclodextrin Inclusion Complexes as Potential Oxygen Delivery Vehicles in Tissue Engineering. *Journal of Biomaterials and Tissue Engineering* **2014**, *4* (11), 957−966.
(13) Xiong, Y.; Liu, Z. Z.; Georgieva, R.; Smuda, K.; Steffen, A.; Sendeski, M.; Voigt, A.; Patzak, A.; Baumler, H. Nonvasoconstrictive Hemoglobin Particles as Oxygen Carriers. *ACS Nano* **2013**, *7* (9), 7454−7461.
(14) Seifu, D. G.; Isimjan, T. T.; Mequanint, K. Tissue engineering scaffolds containing embedded fluorinated-zeolite oxygen vectors. *Acta Biomaterialia* **2011**, *7* (10), 3670−3678.
(15) Lee, H. Y.; Kim, H. W.; Lee, J. H.; Oh, S. H. Controlling oxygen release from hollow microparticles for prolonged cell survival under hypoxic environment. *Biomaterials* **2015**, *53*, 583−591.
(16) Seekell, R. P.; Lock, A. T.; Peng, Y.; Cole, A. R.; Perry, D. A.; Kheir, J. N.; Polizzotti, B. D. Oxygen delivery using engineered microparticles. *Proc. Natl. Acad. Sci. U.S.A.* **2016**, *113* (44), 12380−12385.
(17) Suvarnapathaki, S.; Wu, X.; Lantigua, D.; Nguyen, M. A.; Camci-Unal, G. Breathing life into engineered tissues using oxygen-releasing biomaterials. *NPG Asia Mater.* **2019**, *11*, 65.
(18) Liu, L. H.; Zhang, Y. H.; Qiu, W. X.; Zhang, L.; Gao, F.; Li, B.; Xu, L.; Fan, J. X.; Li, Z. H.; Zhang, X. Z. Dual-Stage Light Amplified Photodynamic Therapy against Hypoxic Tumor Based on an O-2 Self-Sufficient Nanoplatform. *Small* **2017**, *13* (37), No. 1701621.
(19) Zhang, M. G.; Kiratiwongwan, T.; Shen, W. Oxygen-releasing polycaprolactone/calcium peroxide composite microspheres. *Journal of Biomedical Materials Research Part B-Applied Biomaterials* **2020**, *108* (3), 1097−1106.
(20) Zhao, B.; He, J.; Wang, F.; Xing, R.; Sun, B.; Zhou, Y. Polyacrylamide-Sodium Alginate Hydrogel Releasing Oxygen and Vitamin C Promotes Bone Regeneration in Rat Skull Defects. *Front. Mater.* **2021**, *8*, No. 758599.
(21) Majeed, F.; Razzaq, A.; Rehmat, S.; Azhar, I.; Mohyuddin, A.; Rizvi, N. B. Enhanced dye sequestration with natural polysaccharides-based hydrogels: A review. *Carbohydr. Polym.* **2024**, *330*, No. 121820.
(22) Hong, F.; Qiu, P.; Wang, Y.; Ren, P.; Liu, J.; Zhao, J.; Gou, D. Chitosan-based hydrogels: From preparation to applications, a review. *Food Chem. X* **2024**, *21*, No. 101095.
(23) Pal, I.; Pathak, N. K.; Majumdar, S.; Lepcha, G.; Dey, A.; Yatirajula, S. K.; Tripathy, U.; Dey, B. Comparative Vision of Nonlinear Thermo-Optical Features and Third-Order Susceptibility of Mechanically Flexible Metallosupramolecular Self-Repairing Networks with Isomeric Organic Acids. *Inorg. Chem.* **2024**, *63* (26), 12003−12016.
(24) Pal, B.; Majumdar, S.; Pal, I.; Lepcha, G.; Dey, A.; Ray, P. P.; Dey, B. Comparative outcomes of the voltage-dependent current density, charge transportation and rectification ratio of electronic devices fabricated using mechanically flexible supramolecular networks. *Dalton Trans* **2024**, *53* (18), 7912−7921.
(25) Dey, B.; Mondal, R. K.; Mukherjee, S.; Satpati, B.; Mukherjee, N.; Mandal, A.; Senapati, D.; Sinha Babu, S. P. A supramolecular hydrogel for generation of a benign DNA-hydrogel. *RSC Adv.* **2015**, *5* (128), 105961−105968.
(26) Dey, B.; Mukherjee, S.; Mukherjee, N.; Mondal, R. K.; Satpati, B.; Babu, S. P. S. Polyphenol oxidase-based luminescent enzyme hydrogel: an efficient redox active immobilized scaffold. *Bull. Mater. Sci.* **2018**, *41* (1), 14.
(27) Wang, S.; Zheng, H.; Zhou, L.; Cheng, F.; Liu, Z.; Zhang, H.; Wang, L.; Zhang, Q. Nanoenzyme-Reinforced Injectable Hydrogel for Healing Diabetic Wounds Infected with Multidrug Resistant Bacteria. *Nano Lett.* **2020**, *20* (7), 5149−5158.
(28) Lepcha, G.; Sahu, R.; Majumdar, S.; Banerjee, S.; Bhowmick, A.; Sen, S.; Panda, B.; Dhak, D.; Sarkar, K.; Dey, B. MoS 2 and MoSe 2 2D nanosheets-based supramolecular nanostructure scaffold-capped Ag-NPs: exploring their morphological, anti-bacterial, and anticancer properties. *New J. Chem.* **2023**, *47* (32), 15357−15365.
(29) Majumdar, S.; Ghosh, M.; Mukherjee, S.; Satpati, B.; Dey, B. DNA mediated graphene oxide (GO)-nanosheets dispersed supramolecular GO-DNA hydrogel: An efficient soft-milieu for simplistic synthesis of Ag-NPs@GO-DNA and Gram plus ve/-ve bacteria-based Ag-NPs@GO-DNA-bacteria nano-bio composites. *J. Mol. Liq.* **2021**, *342*, No. 117482.
(30) Kawashima, A.; Sekizawa, A.; Koide, K.; Hasegawa, J.; Satoh, K.; Arakaki, T.; Takenaka, S.; Matsuoka, R. Vitamin C Induces the Reduction of Oxidative Stress and Paradoxically Stimulates the Apoptotic Gene Expression in Extravillous Trophoblasts Derived From First-Trimester Tissue. *Reprod Sci.* **2015**, *22* (7), 783−90.
(31) Shang, F.; Lu, M.; Dudek, E.; Reddan, J.; Taylor, A. Vitamin C and vitamin E restore the resistance of GSH-depleted lens cells to H2O2. *Free Radic Biol. Med.* **2003**, *34* (5), 521−30.
(32) Yang, H.; Wu, S.; Feng, R.; Huang, J.; Liu, L.; Liu, F.; Chen, Y. Vitamin C plus hydrogel facilitates bone marrow stromal cell-mediated endometrium regeneration in rats. *Stem Cell Res. Ther.* **2017**, *8* (1), 267.
(33) Lu, Z.; Jiang, X.; Chen, M.; Feng, L.; Kang, Y. J. An oxygen-releasing device to improve the survival of mesenchymal stem cells in tissue engineering. *Biofabrication* **2019**, *11* (4), No. 045012.
(34) Khodaveisi, J.; Banejad, H.; Afkhami, A.; Olyaie, E.; Lashgari, S.; Dashti, R. Synthesis of calcium peroxide nanoparticles as an

https://doi.org/10.1021/acsomega.4c06642
ACS Omega 2024, 9, 47585−47596

innovative reagent for in situ chemical oxidation. *J. Hazard Mater.* **2011**, *192* (3), 1437−40.
(35) Alves, A. L.; Carvalho, A. C.; Machado, I.; Diogo, G. S.; Fernandes, E. M.; Castro, V. I. B.; Pires, R. A.; Vázquez, J. A.; Pérez-Martín, R. I.; Pérez-Martín, M.; Reis, R. L.; Silva, T. H. Cell-Laden Marine Gelatin Methacryloyl Hydrogels Enriched with Ascorbic Acid for Corneal Stroma Regeneration. *Bioengineering* **2023**, *10* (1), 62.
(36) Ghahremani-Nasab, M.; Akbari-Gharalari, N.; Rahmani Del Bakhshayesh, A.; Ghotaslou, A.; Ebrahimi-Kalan, A.; Mahdipour, M.; Mehdipour, A. Synergistic effect of chitosan-alginate composite hydrogel enriched with ascorbic acid and alpha-tocopherol under hypoxic conditions on the behavior of mesenchymal stem cells for wound healing. *Stem Cell Res. Ther.* **2023**, *14* (1), 326.
(37) Han, Y. W. Fusobacterium nucleatum: a commensal-turned pathogen. *Curr. Opin Microbiol* **2015**, *23*, 141−7.
(38) Socransky, S. S.; Haffajee, A. D.; Cugini, M. A.; Smith, C.; Kent, R. L., Jr. Microbial complexes in subgingival plaque. *J. Clin Periodontol* **1998**, *25* (2), 134−44.
(39) Byrd, K. M.; Gulati, A. S. The ″Gum-Gut″ Axis in Inflammatory Bowel Diseases: A Hypothesis-Driven Review of Associations and Advances. *Front Immunol* **2021**, *12*, No. 620124.
(40) Pan, W.; Wang, Q.; Chen, Q. The cytokine network involved in the host immune response to periodontitis. *Int. J. Oral Sci.* **2019**, *11* (3), 30.
(41) Stadler, A. F.; Angst, P. D.; Arce, R. M.; Gomes, S. C.; Oppermann, R. V.; Susin, C. Gingival crevicular fluid levels of cytokines/chemokines in chronic periodontitis: a meta-analysis. *J. Clin Periodontol* **2016**, *43* (9), 727−45.
(42) Ebersole, J. L.; Kirakodu, S.; Novak, M. J.; Stromberg, A. J.; Shen, S.; Orraca, L.; Gonzalez-Martinez, J.; Burgos, A.; Gonzalez, O. A. Cytokine gene expression profiles during initiation, progression and resolution of periodontitis. *J. Clin Periodontol* **2014**, *41* (9), 853−61.
(43) De Benedetti, F.; Rucci, N.; Del Fattore, A.; Peruzzi, B.; Paro, R.; Longo, M.; Vivarelli, M.; Muratori, F.; Berni, S.; Ballanti, P.; Ferrari, S.; Teti, A. Impaired skeletal development in interleukin-6-transgenic mice: a model for the impact of chronic inflammation on the growing skeletal system. *Arthritis Rheum* **2006**, *54* (11), 3551−63.
(44) Wu, Q.; Zhou, X.; Huang, D.; Ji, Y.; Kang, F. IL-6 Enhances Osteocyte-Mediated Osteoclastogenesis by Promoting JAK2 and RANKL Activity In Vitro. *Cell Physiol Biochem* **2017**, *41* (4), 1360−1369.
(45) Ben-Sasson, S. Z.; Hu-Li, J.; Quiel, J.; Cauchetaux, S.; Ratner, M.; Shapira, I.; Dinarello, C. A.; Paul, W. E. IL-1 acts directly on CD4 T cells to enhance their antigen-driven expansion and differentiation. *Proc. Natl. Acad. Sci. U. S. A.* **2009**, *106* (17), 7119−24.
(46) Gilowski, L.; Wiench, R.; Płocica, I.; Krzemiński, T. F. Amount of interleukin-1β and interleukin-1 receptor antagonist in periodontitis and healthy patients. *Arch Oral Biol.* **2014**, *59* (7), 729−34.
(47) Górska, R.; Gregorek, H.; Kowalski, J.; Laskus-Perendyk, A.; Syczewska, M.; Madaliński, K. Relationship between clinical parameters and cytokine profiles in inflamed gingival tissue and serum samples from patients with chronic periodontitis. *J. Clin Periodontol* **2003**, *30* (12), 1046−52.
(48) Madureira, D. F.; Lima, I. L. D. A.; Costa, G. C.; Lages, E. M. B.; Martins, C. C.; Da Silva, T. A. Tumor Necrosis Factor-alpha in Gingival Crevicular Fluid as a Diagnostic Marker for Periodontal Diseases: A Systematic Review. *J. Evid. Based Dent. Pract.* **2018**, *18* (4), 315−331.
(49) Basso, F. G.; Pansani, T. N.; Turrioni, A. P.; Soares, D. G.; de Souza Costa, C. A.; Hebling, J. Tumor Necrosis Factor-α and Interleukin (IL)-1β, IL-6, and IL-8 Impair In Vitro Migration and Induce Apoptosis of Gingival Fibroblasts and Epithelial Cells, Delaying Wound Healing. *J. Periodontol* **2016**, *87* (8), 990−6.
(50) Arancibia, R.; Oyarzún, A.; Silva, D.; Tobar, N.; Martínez, J.; Smith, P. C. Tumor necrosis factor-α inhibits transforming growth factor-β-stimulated myofibroblastic differentiation and extracellular matrix production in human gingival fibroblasts. *J. Periodontol* **2013**, *84* (5), 683−93.
(51) Assuma, R.; Oates, T.; Cochran, D.; Amar, S.; Graves, D. T. IL-1 and TNF antagonists inhibit the inflammatory response and bone loss in experimental periodontitis. *J. Immunol* **1998**, *160* (1), 403−9.

https://doi.org/10.1021/acsomega.4c06642
ACS Omega 2024, 9, 47585−47596